

**A BN Anthracene Mimics the Electronic Structure of More Highly Conjugated Systems**

Journal:	<i>Dalton Transactions</i>
Manuscript ID	DT-ART-01-2019-000481
Article Type:	Paper
Date Submitted by the Author:	31-Jan-2019
Complete List of Authors:	Ishibashi, Jacob; Boston College, Merkert Chemistry Centre Darrigan, Clovis; Université de Pau et des Pays de l'Adour, Equipe Chimie Physique, IPREM, UMR 5254 Chrostowska, Anna; Université de Pau et des Pays de l'Adour, Equipe Chimie Physique, IPREM, UMR 5254 Li, Bo; Boston College, Chemistry Liu, Shih-Yuan; Boston College, Merkert Chemistry Centre



Journal Name

ARTICLE

A BN Anthracene Mimics the Electronic Structure of More Highly Conjugated Systems†

Jacob S. A. Ishibashi,^{a,c} Clovis Darrigan,^b Anna Chrostowska,^b Bo Li,^a and Shih-Yuan Liu^{*a}

Received 00th January 20xx,
Accepted 00th January 20xx

DOI: 10.1039/x0xx00000x

www.rsc.org/

9a,9-BN Anthracene was synthesized using a simple three-step sequence involving intramolecular electrophilic borylation of 2-benzylpyridines. The same procedure can be applied to yield a number of substituted 9a,9-BN anthracenes. Spectroscopic characterization of the parental compound (UV-photoelectron spectroscopy, UV-vis absorption/emission) shows an electronic structure more similar to that of a larger conjugated system rather than anthracene, the direct all-carbon analogue.

Introduction

In the field of organic-based electronics, devices incorporating acenes are some of the highest-performing.¹ Modulating the electronic structures of acenes requires substituting the acene periphery or changing conjugation length.² As conjugation length of acenes increases, their applicability in optoelectronic devices also increases,³ but their synthetic accessibility and solubility often decrease. If smaller, less conjugated structures could be made to mimic the electronic structures of longer acenes, those two limitations of highly conjugated acenes might be alleviated.

BN/CC isosterism has emerged as a useful design strategy for modulating the optoelectronic properties of conjugated polycyclic aromatic hydrocarbons (PAHs).⁴ When replacing carbon atoms in the acene skeleton with boron-nitrogen units, it is theoretically possible to tune electronic structure simply by changing the location or orientation of the BN units. Two exemplary studies by Müllen and co-workers and by Piers and co-workers show that different isomers of non-acene BN π -conjugated molecules have markedly different electronic properties from one another.⁵ In the context of acenes, we showed that judicious choice of BN unit placement at the 9- and 1-positions within the naphthalene scaffold resulted in an electronic structure resembling that of a more conjugated molecule, anthracene (Fig. 1, top).⁶ To demonstrate that smaller BN acenes can mimic the electronic structures of larger, more device-relevant, conjugated systems, we present here the

synthesis and characterization of 9a,9-BN anthracene **1** and its substituted derivatives.

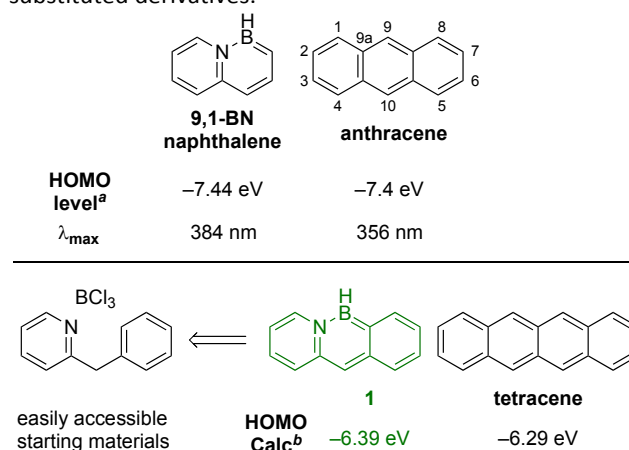


Fig. 1 Mimicking the electronic structure of higher all-carbon acenes with less conjugated BN acenes. ^aDetermined by UV-PES. BN naphthalene data taken from ref. 6 Anthracene data taken from ref. 18. ^bCalculated at the CAM-B3LYP/6-311G(d,p) level.

Results and Discussion

Synthesis of 9a,9-BN Anthracene *via* Electrophilic Borylation

After analyzing the predicted electronic properties of the entire BN anthracene series,⁷ we chose to target 9a,9-BN anthracene **1** since it is calculated to have a HOMO energy level similar to that of the carbonaceous tetracene (Fig. 1, bottom) and seemed to be easily accessible synthetically. Previously synthesized BN naphthalenes^{6,8} (Scheme 1a) map onto our target **1**, but the reaction sequences required to obtain **1** from these BN naphthalenes would likely be unwieldy and inefficient. For example, Cui's synthetic method for substituted 2,1-BN naphthalenes requires a carbon-based substituent at the nitrogen atom (R¹ = aryl) and at the adjacent carbon (R³ = alkyl or aryl), and these types of substituents cannot readily be transformed into other functional groups for the synthesis of **1**.

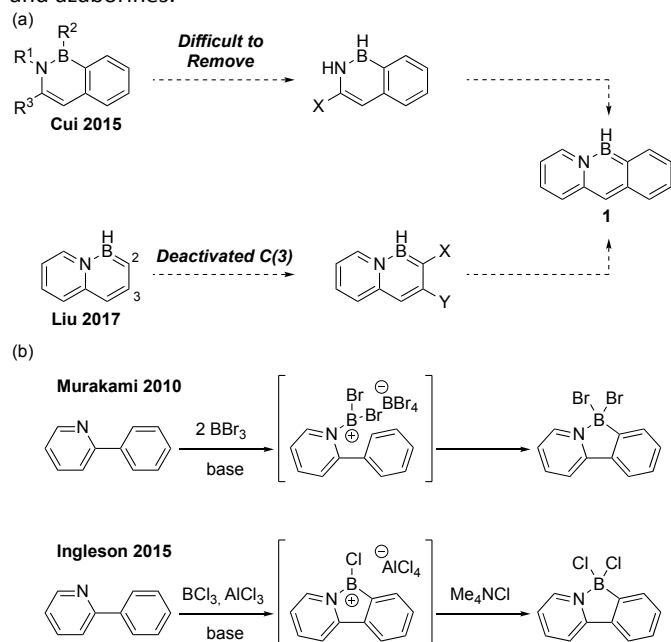
^a Department of Chemistry, Merkert Chemistry Center, Boston College, Chestnut Hill, Massachusetts 02467, United States.

^b CNRS and the Energy and Environment Solutions Initiative (E2S) at Université de Pau et des Pays de l'Adour, and Institut des Sciences Analytiques et de Physico-Chimie pour l'Environnement et les Matériaux, UMR 5254, 64000, Pau, France.

^c Current address: Department of Chemistry, Northwestern University, Evanston, Illinois, 60208 United States.

†Electronic Supplementary Information (ESI) available: Experimental, computational, and crystallographic information. See DOI: 10.1039/x0xx00000x

On the other hand, our group disclosed the synthesis of 9,1-BN naphthalene but did not demonstrate further functionalization. Selective substitution of the 2- and 3-positions is required for benzannulation of this scaffold through conventional synthetic methods such as ring-closing metathesis-oxidation.⁹ However, naphthalene EAS occurs preferentially at the alpha sites over the beta sites, and EAS of azaborines occurs preferentially at the position adjacent to boron. The 3-position, therefore, is probably deactivated to electrophilic aromatic substitution (EAS) reactions with respect to both the naphthalene skeleton and azaborines.

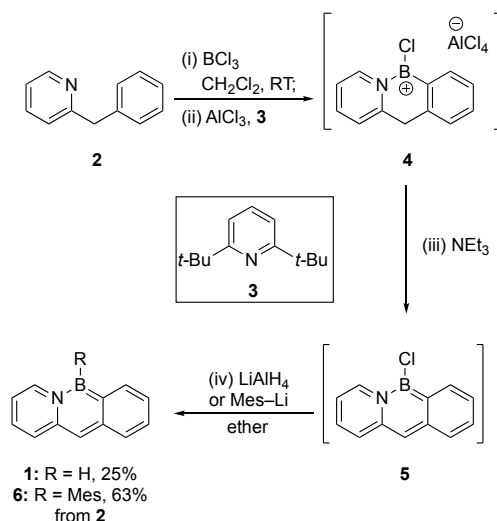


Scheme 1 (a) Synthetic plans toward **1** from known BN naphthalenes may be difficult due to limitations in the previously synthesized structures. (b) Borenium-mediated cyclization efficiently creates fused ring systems.

To synthesize compound **1**, it may be more effective to investigate new chemistry than to elaborate existing structures. We envisioned using electrophilic C–H borylation chemistry recently employed by the groups of both Murakami and Ingleson to give 5-membered rings (Scheme 1b).¹⁰ A key difference between the “Murakami-Ingleson” system and our target **1** is that the boron atom in **1** is tricoordinate instead of tetracoordinate. It is thus more likely for the substituents on the boron atom in **1** to become an integral part of the conjugation path instead of simply planarizing the system and providing an inductive influence on electronic structure.^{11,12}

We began the synthesis of **1** by treating commercially-available 2-benzylpyridine **2** successively with boron trichloride, aluminum chloride, and the bulky base 2,6-di-*tert*-butylpyridine **3** (Scheme 2a). This resulted in an intermediate with ¹H NMR resonances shifted downfield from those of the starting material, and the ¹¹B NMR (δ 46 (s)) was consistent with an annulated, borenium-centered **4** (See Supporting Information (SI), Fig. S-1 and S-2). Instead of intercepting borenium **4** with a chloride anion to obtain a neutral, cyclic pyridine-borane similar to the one produced by Ingleson and co-workers^{10b} (Scheme 1b), we continued the one-pot sequence by treating the

reaction mixture with triethylamine to obtain aromatic BN anthracene **5** (¹¹B NMR δ 35 (s)). We subsequently treated **5** with lithium aluminum hydride to give the parental BN anthracene **1**. The crystal structure of **1** is disordered, and the molecules pack with a herringbone motif, much like all-carbon anthracene (See SI, Fig. S-10).¹³ Fortunately, a mesitylated derivative **6**, which can be synthesized on gram scale using a similar route, gave an unambiguous crystal structure (Fig. 2, right).¹⁴



Scheme 2 Synthetic route to 9a,9-BN anthracenes.

Structural Comparison with 1,2-BN Anthracene

Figure 2 shows a comparison of the crystal structure of **6** to that of the 1,2-BN anthracene isomer **X-Mes** reported by Klausen and co-workers.¹⁵ Compound **6** displays similar BN-ring planarity to B-mesityl-1,2-BN anthracene **X-Mes**. The root-mean square (RMS) deviation from the mean plane formed by the BN-containing ring of **6** are both 0.007 Å indicating good planarity for both rings.

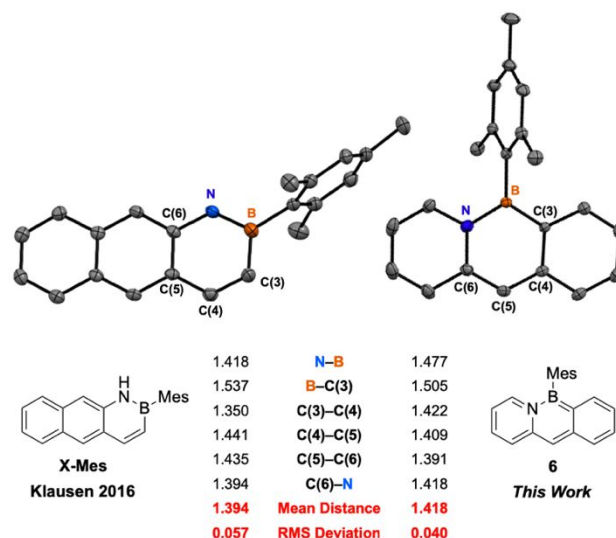


Fig. 2 X-ray crystal structure comparison between two isomers of BN anthracene. Hydrogen atoms are omitted for clarity. Data for **X-Mes** taken from ref 15.

However, the BN-containing ring's bond lengths differ significantly between the two BN anthracene isomers. For **6**, the boron-nitrogen bond distance of 1.477 Å is longer than that of **X-Mes** (1.418 Å). Both distances are longer than expected for a B=N bond (approximate maximum: 1.408 Å), but shorter than expected for a B–N dative interaction (approximate minimum: 1.601 Å).¹⁶ In contrast, the intra-ring boron-carbon distance of 1.505 Å for **6** is significantly shorter than that in **X-Mes** (1.537 Å). Additionally, the C(3)–C(4) distance in **X-Mes** is exceedingly short (1.350 Å), but the corresponding distance in **6** is much longer (1.422 Å). The RMS deviation from the mean ring bond length for **6** is 0.040 Å, while that for **X-Mes** is 0.057 Å. These relatively homogenized bond distances for the BN-containing ring in **6** suggest increased electronic delocalization as compared to the BN-containing ring of **X-Mes**. In support of this, nucleus independent chemical shift (NICS) calculations for the BN-containing ring of **6** show a more negative NICS(0) value (–6.92) than the BN ring in **X-Mes** (–3.07) indicating more electronic delocalization for **6** than for **X-Mes** (Fig. S-3).

Spectroscopic Characterization

We performed UV-photoelectron spectroscopy (UV-PES) on **1** to determine the energies of its occupied orbitals (Fig. 3). This technique employs ultraviolet radiation to eject electrons from occupied orbitals including the HOMO, and we have used it to investigate a wide variety of BN aromatic compounds.¹⁷ The opposite of the energy of a given band is taken to be the energy of the orbital from which an electron has been ejected. Importantly, we can directly compare **1** to our previously synthesized 1,2-BN anthracene and also to the all-carbon analogue.¹⁸ Compound **1** has a higher-lying HOMO (–7.04 eV) than both 1,2-BN anthracene (–7.7 eV) and all-carbon anthracene (–7.4 eV). This result shows that the HOMO of **1** is energetically more similar to that of tetracene (HOMO by PES = –7.04 eV)¹⁹ than that of anthracene.

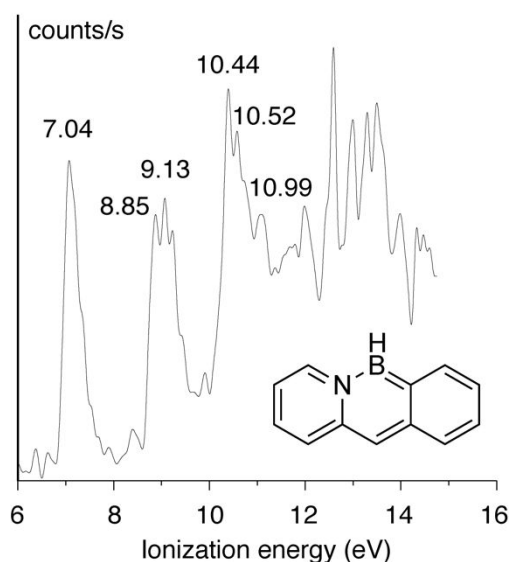


Fig. 3 UV-photoelectron spectrum of **1**.

Next, we investigated the optical properties of **1**. While the previously synthesized 1,2-BN anthracene absorbs and emits in

the ultraviolet (like anthracene itself), **1** has absorption and emission in the visible range. The absorption spectrum of **1** in cyclohexane ($\lambda_{\text{max}} = 437 \text{ nm}$, Fig. 4)²⁰ is bathochromically shifted from that of all-carbon anthracene ($\lambda_{\text{max}} = 356 \text{ nm}$) and that of the previously synthesized parent 1,2-BN anthracene **X-H** ($\lambda_{\text{max}} = 359 \text{ nm}$) and slightly hypsochromically shifted from that of tetracene ($\lambda_{\text{max}} = 473 \text{ nm}$).

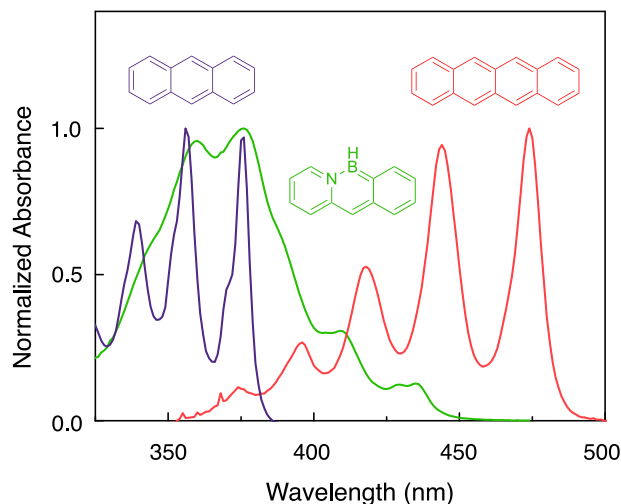


Fig. 4 Normalized absorbance spectra for anthracene (purple), BN anthracene **1** (green), and tetracene (red) obtained in cyclohexane solution.

Theoretical calculations may help to elucidate the spectral differences between BN anthracene parental structures **1** and **X-H**. The relatively large overlap between the HOMO and LUMO coefficients for **1** and also for **X-H** (Fig. 5) suggest that little charge transfer character, if any, should be expected from the HOMO-LUMO transition for either molecule. TD-DFT calculations performed at the B3LYP/6-311G(d,p) suggest that the lowest-energy absorption band for both molecules corresponds to the HOMO-LUMO transition (See SI p. S-17 for calculation details and Figure S4 and S5 for simulated spectra for **1** and **X-H**, respectively). The lower HOMO-LUMO gap of **1** versus both anthracene and the 1,2-BN anthracene isomer observed using UV-visible absorption spectroscopy is further evidence for greater electronic delocalization implied by the homogenized bond lengths observed in our crystallography study.

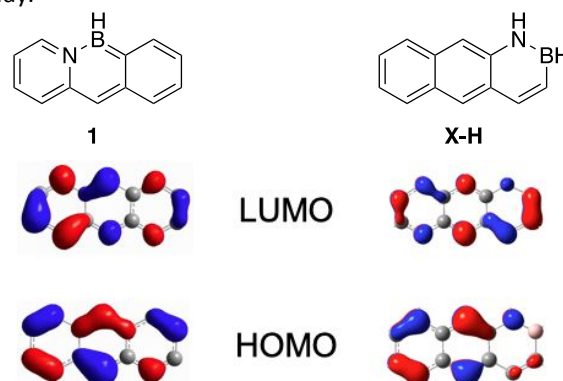


Fig. 5. HOMO and LUMO coefficients of **6** and **X-H** calculated at the CAM-B3LYP/6-311G(d,p) level.

The emission of **1** is blue ($\lambda_{em} = 475$ nm, $\Phi_{pl} = 0.32$, See SI, Fig. S-8), while mesitylated compound **6** has blue-green emission in cyclohexane solution ($\lambda_{em} = 483$ nm, $\Phi_{pl} = 0.32$, Fig. 6). After solution-casting a thin film of **6** on a glass slide, we collected an emission spectrum, which strongly resembled the solution-phase data. Peak emission of the film is bathochromically shifted by only 85 cm^{-1} with respect to that of the solution ($\lambda_{em} = 487$ nm), and the film has a photoluminescence quantum yield of 0.85 which is much greater than that measured in solution.²¹

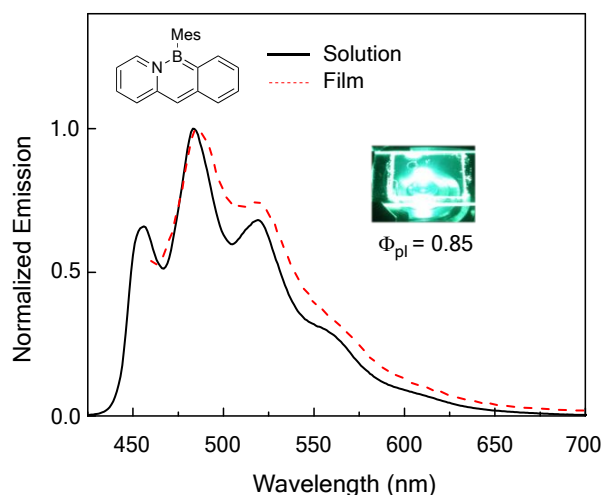
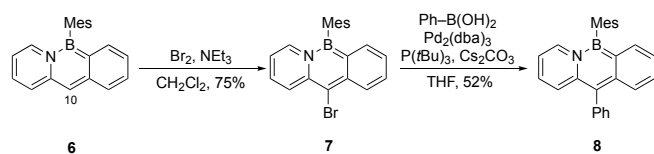


Fig. 6 Emission spectra of compound **6** from cyclohexane solution and from thin film. Photo: the color of emission from the thin film of **6**.

Structural and Electronic Diversification of 9a,9-BN Anthracenes

To explore the possibility of modifying the electronic structure of the 9a,9-BN anthracene scaffold by derivatization, we treated **6** with bromine in the presence of triethylamine. This EAS reaction is selective for the apical 10-position (Scheme 3). The halogenated compound **7** allows for arylation of the BN anthracene core *via* Suzuki-Miyaura coupling.

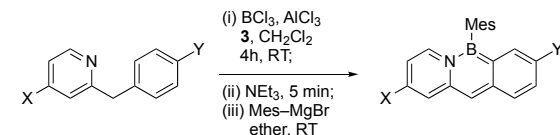


Scheme 3 Elaboration of the 9,9a-BN anthracene scaffold

Other positions of the core cannot easily be substituted by EAS but they can be targeted simply through our bottom-up synthetic approach. Table 1 shows various substituted derivatives of **6** we synthesized using our general synthetic procedure (see Scheme 2a) along with their absorption and emission properties. These substitutions give rise to significant spectral shifts. Both λ_{max} and λ_{em} bathochromically shift as we impart stronger donor-acceptor character through substitution. For example, methoxy- and chloro-substituted compound **12** shows a 979 cm^{-1} and 1250 cm^{-1} bathochromic shift in λ_{max} and λ_{em} , respectively (See SI, Fig. S-7 and S-8 for absorption and emission spectra). Our conditions tolerate chlorinated and

methoxylated substrates but not stronger donors such as dimethylamine or stronger withdrawing groups such as fluorine or nitrile.²²

Table 1 Bottom-up synthesis of substituted BN anthracenes and associated optical properties of the products.



Compound	X =	Y =	Yield	$\lambda_{max(abs)}^b$	$\lambda_{max(em)}^c$	Φ_{pl}^d
6	H	H	63% ^a	442 nm	483 nm	0.32
9	H	Cl	44%	444 nm	482 nm	0.27
10	H	OMe	9%	447 nm	496 nm	0.60
11	Cl	H	40%	458 nm	496 nm	0.17
12	Cl	OMe	33%	462 nm	514 nm	0.33

^a Mesityllithium used as the nucleophile. ^b Peak of lowest-energy absorption band.

^c Peak of highest-intensity emission. ^d Absolute quantum yield from cyclohexane solution determined using an integrating sphere.

Conclusions

In summary, we have developed a simple one-pot synthesis of a novel family of BN anthracenes, i.e., 9a,9-BN anthracene, that exhibits optoelectronic properties associated with a larger carbonaceous acene. We characterized the parental 9a,9-BN anthracene **1** by UV-photoelectron spectroscopy and optical absorption and emission spectroscopy, finding that **1** is electronically more similar to a more conjugated species such as tetracene than it is to its 1,2-BN anthracene isomer or its direct, all-carbon analogue, anthracene. This study further demonstrates that strategic BN unit placement within an acene holds promise in diversifying the electronic structure of acenes without changing the topology of the system.

Conflicts of interest

There are no conflicts to declare.

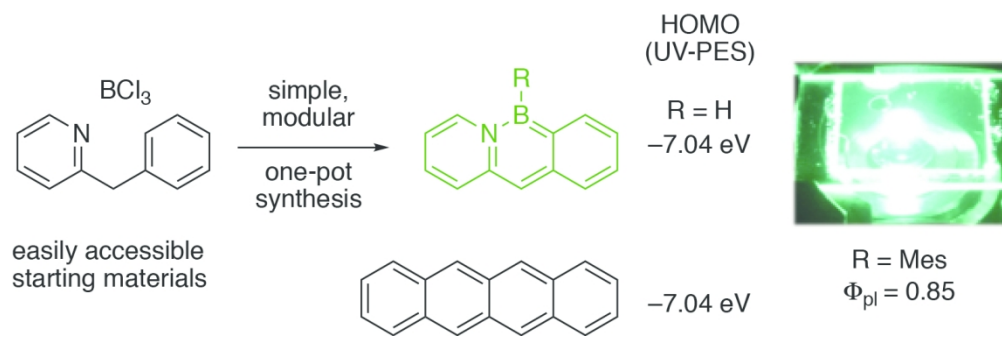
Acknowledgements

This work was supported by the National Science Foundation (CHE-1561153). J.S.A.I. thanks the LaMattina Family Graduate Fellowship in Chemical Synthesis for support and Dr. F. Haefner for guidance in computational chemistry. A.C. thanks the E2S initiative for support.

Notes and references

- For a review on acenes in organic field-effect transistors, see: H. Sirringhaus, *Adv. Mater.* 2014, **26**, 1319–1335.

- 2 A. Naibi Lakshminarayana, A. Ong and A. Chi, *J. Mater. Chem. C* 2018, **6**, 3551–3563.
- 3 A typical organic semiconductor bandgap is 2–3 eV. J. Zaumseil and H. Sirringhaus, *Chem. Rev.* 2007, **107**, 1296–1323. Visible light has an energy range of 3.1–1.6 eV.
- 4 For recent reviews, see: (a) X.-Y. Wang, J.-Y. Wang and J. Pei, *Chem. Eur. J.* 2015, **21**, 3528–3539. (b) M. M. Morgan and W. E. Piers, *Dalton Trans.* 2016, **45**, 5920–5924. (c) J. H. Barnard, S. Yruegas, K. Huang and C. D. Martin, *Chem. Commun.* 2016, **52**, 9985–9991. (d) G. Belanger-Chabot, H. Braunschweig and D. K. Roy, *Eur. J. Inorg. Chem.* 2017, 4353–4368. (e) Z. X. Giustra and S.-Y. Liu, *J. Am. Chem. Soc.* 2018, **140**, 1184–1194. (f) J. Huang and Y. Li, *Front. Chem.* 2018, **6**, 341.
- 5 (a) X.-Y. Wang, A. Narita, X. Feng and K. Müllen, *J. Am. Chem. Soc.* 2015, **137**, 7668–7671. (b) M. J. D. Bosdet, C. A. Jaska, W. E. Piers, T. S. Sorensen and M. Parvez, *Org. Lett.* 2007, **9**, 1395–1398.
- 6 Z. Liu, J. S. A. Ishibashi, C. Darrigan, A. Dargelos, A. Chrostowska, B. Li, M. Vasiliu, D. A. Dixon and S.-Y. Liu, *J. Am. Chem. Soc.* 2017, **139**, 6082–6085.
- 7 J. S. A. Ishibashi, A. Dargelos, C. Darrigan, A. Chrostowska and S.-Y. Liu, *Organometallics* 2017, **36**, 2494–2497.
- 8 X. Liu, P. Wu, J. Li and C. Cui *J. Org. Chem.* 2015, **80**, 3737–3744.
- 9 (a) X. Fang, H. Yang, J. W. Kampf, M. M. Banaszak Holl and A. J. Ashe, III *Organometallics* 2006, **25**, 513–518. (b) A. D. Rohr, J. W. Kampf, A. J. Ashe, III. *Organometallics* 2014, **33**, 1318–1321.
- 10 (a) N. Ishida, T. Moriya, T. Goya and M. Murakami, *J. Org. Chem.* 2010, **75**, 8709–8712. (b) D. L. Crossley, J. Cid, L. D. Curless, M. L. Turner and M. J. Ingleson, *Organometallics* 2015, **34**, 5767–5774.
- 11 Recent examples of conjugated systems bearing BN units with tetrahedral boron bridges: (a) C. Zhu, Z.-H. Guo, A. U. Mu, Y. Liu, S. E. Wheeler and L. Fang, *J. Org. Chem.* 2016, **81**, 4347–4352. (b) M. Grandl, T. Kaese, A. Krautsieder, Y. Sun and F. Pammer, *Chem. - Eur. J.* 2016, **22**, 14373–14382. (c) D. L. Crossley, R. Goh, J. Cid, I. Vitorica-Yrezabal, M. L. Turner and M. J. Ingleson, *Organometallics* 2017, **36**, 2597–2604. (d) Q. Hou, L. Liu, S. K. Møllerup, N. Wang, T. Peng, P. Chen and S. Wang, *Org. Lett.* 2018, **20**, 6467–6470. (e) K. Liu, R. A. Lalancette and F. Jäkle, *J. Am. Chem. Soc.* 2017, **139**, 18170–18173.
- 12 Recent examples of conjugated systems bearing BN units with trigonal boron atoms: (a) C. Li, Y. Liu, Z. Sun, J. Zhang, M. Liu, C. Zhang, Q. Zhang, H. Wang and X. Liu, *Org. Lett.* 2018, **20**, 2806–2810. (b) M. M. Morgan, E. A. Patrick, J. M. Rautiainen, H. M. Tuononen, W. E. Piers and D. M. Spasyuk, *Organometallics* 2017, **36**, 2541–2551. (c) D.-T. Yang, Y. Shi, T. Peng and S. Wang, *Organometallics* 2017, **36**, 2654–2660.
- 13 Anthracene packs in the herringbone motif: J. M. Robertson, *Proc. R. Soc. Lond.* 1933, **140**, 79–98.
- 14 Two molecules of **6** pack in the unit cell. Therefore, all measurements of **6** quoted in the text are the average of the two molecules.
- 15 H. L. van de Wouw, J. Y. Lee, M. A. Siegler and R. S. Klausen, *Org. Biomol. Chem.* 2016, **14**, 3256–3263.
- 16 F. H. Allen, O. Kennard, D. G. Watson, L. Brammer, A. G. Orpen and R. Taylor, *J. Chem. Soc., Perkin Trans. 2* 1987, S1–S17.
- 17 Examples include: (a) A. Chrostowska, M. Maciejczyk, A. Dargelos, P. Baylère, L. Weber, V. Werner, D. Eickhoff, H. G. Stammer and B. Neumann, *Organometallics* 2010, **29**, 5192–5198. (b) A. Chrostowska, S. Xu, A. N. Lamm, A. Mazière, C. D. Weber, A. Dargelos, P. Baylère, A. Graciaa and S.-Y. Liu, *J. Am. Chem. Soc.* 2012, **134**, 10279–10285. (c) A. Chrostowska, S. Xu, A. Mazière, K. Boknevit, B. Li, E. R. Abbey, A. Dargelos, A. Graciaa and S.-Y. Liu, *J. Am. Chem. Soc.* 2014, **136**, 11813–11820. (d) C. R. McConnell, P. G. Campbell, C. R. Fristoe, P. Memmel, L. N. Zakharov, B. Li, C. Darrigan, A. Chrostowska and S.-Y. Liu, *Eur. J. Inorg. Chem.* 2017, 2207–2210.
- 18 J. S. A. Ishibashi, J. L. Marshall, A. Mazière, G. J. Lovinger, B. Li, L. N.; Zakharov, A. Dargelos, A. Graciaa, A. Chrostowska and S.-Y. Liu, *J. Am. Chem. Soc.* 2014, **136**, 15414–15421.
- 19 E. Clar and W. Schmidt, *Tetrahedron* 1975, **31**, 2263–2271.
- 20 λ_{max} of absorption is defined here as the lowest energy absorption band associated with the HOMO-LUMO transition, i.e., excitation to the S_1 state. See Electronic Supporting Information for the assignment by TD-DFT calculations.
- 21 Φ_{pi} is inversely proportional to the non-radiative decay rate constant k_{nr} . The value of k_{nr} can be increased by collision with quenchers or when vibrational modes become more available. Both collisions with quenchers and the number of available vibrational modes are necessarily increased when a fluorophore is placed in solution versus the solid state. See: J. R. Lakowicz, *Principles of Fluorescence Spectroscopy*, 3rd ed, Springer, New York, 2006.
- 22 Our substrate scope is consistent with previous reports of intramolecular electrophilic C–H borylation: a) V. Bagutski, A.; Del Grosso, J. A.; Carrillo, I. A. Cade, M. D. Helm, J. R. Lawson, P. J. Singleton, S. A. Solomon, T. Marcelli and M. J. Ingleson, *J. Am. Chem. Soc.* 2013, **135**, 474–487. b) A. Del Grosso, M. D. Helm, S. A.; Solomon, D. Caras-Quintero and M. J. Ingleson, *Chem. Commun.* 2011, **47**, 12459–12461.



137x44mm (300 x 300 DPI)